International Journal of Engineering & Technology, 7 (4) (2018) 5580-5588

International Journal of Engineering & Technology

Website: www.sciencepubco.com/index.php/IJET
doi: 10.14419/ijet.v7i4.19247
Research paper

A restricted Boltzmann machine based prostate tumor detection in MRI images

Mohammad Jassim Kredi [1] *, Rabah Nori Farhan [2]

[1] Department of Computer Science, College of Computer Science and Information Technology, University of Anbar, Anbar, Iraq
[2] Assistant Proof. Renewable Energy Research Center, University of Anbar, Anbar, Iraq
**Corresponding author E-mail: mohkredi@gmail.com*

Abstract

Context: Prostate cancer is a common and malignant tumor. Thus, to improve the excellence of life of cancer person is the early diagnosis of prostate cancer. Prostate tumors are divided in terms of growth to: slow growth and often confined to the prostate gland and growing growth and often spread the prostate gland to other members which is the second most regular reason for malignancy in the world According to estimates and studies conducted by the World Health Organization. MRI uses medical imaging technology used on a scale It is widely evaluated for tumors, but the large amount of data produced by MRI can vary greatly. Thus manual detection will be a challenge.
The Problem: The early diagnosis of prostate cancer plays a key role in prolonging the patient's life. as doctors are still human, and rely on factors such as the eye in the diagnosis and these factors do not avoid mistakes in addition to that The wrong diagnosis presents the patient to death, especially the description of inappropriate treatment or surgical intervention (tumor contact) or chemical radiation therapy for this reason completed the diagnosis leads to high accuracy diagnosis, accuracy Diagnosis assumes an imperative job in the fight against the disease. Regular re-diagnosis is important and necessary to ensure that patients survive and keep them away from the risk of disease. However, re-diagnosis and examination often consumes many financial expenses in this regard. This system is designed to assist radiologists in their practice Clinical.
Approach: In this paper, the researcher is interested in focusing on the area of the prostate gland and detecting abnormal cases in the image. The proposed strategy relies on one of the deep learning algorithms Restricted Boltzmann Machine algorithm, and image processing techniques histogram equalization one of Contrast enhancement techniques, to enhance grayscale images It improves the differentiation of pictures by changing the qualities in a force picture so the histogram of the output image approximately matches a specified histogram and extract the features that help us to make the right decision in the process of diagnosis as well as to increase the efficiency of the system and obtain the highest accuracy in the results where the use of dataset images of the magnetic resonance of the prostate, which contains more than 1700 different images of 230 infected and was classified using an algorithm to non-tumor and tumor.
Finding: The results of this study confirmed that this method works effectively. This method was applied to a database containing 1730 medical images. The accuracy of this method was 98.8439. To demonstrate the productivity of the proposed system, the images were entered into a normal neural network. Than Indicates the efficiency of our proposed system.

Keywords: *Prostate Cancer; Magnetic Resonance Imaging; Restricted Boltzmann Machine; Deep Belief Network*

1. Introduction

Since 2012, according to global statistics, prostate cancer ranks second and is one of the most common diseases among men and ranks fourth among cancers for both sexes and is considered a disease that has become a source of concern for public health in the world As per the reports of the World Health Organization, most deaths among men due to this serious disease , Tumors of the prostate in terms of growth to: slow growth and are often limited to the prostate gland and to the rapid growth and often spread out of the prostate gland to other organs and in this manner, early analysis and hazard evaluation play a key role in the treatment of patients and Since 2012 [1 - 3], according to global statistics, prostate cancer ranks second and is one of the most common diseases among men and ranks fourth among cancers for both sexes and is considered a disease that has become a source of concern for public health in the world As per the reports of the World Health Organization, most deaths among men due to this serious disease , Tumors of the prostate in terms of growth to: slow growth and are often limited to the prostate gland and to the rapid growth and often spread out of the prostate gland to other organs and thusly, early conclusion and hazard evaluation play key roles in the treatment of patients, Followed up [3].

In recent years, to improve diagnosis, new imaging procedures dependent on MRI have been created to improve conclusion. In practice, diagnosis can be made of multiple factors such as observational fluctuation, vision and complexity of lesions. In this regard, computer-assisted detection systems are designed to assist radiologists in their clinical practice [4].

In this paper we will classify the prostate to non-tumor (intact) and tumor (infected) after carrying out the preprocessing process and extract the images from the images to improve the accuracy of the results

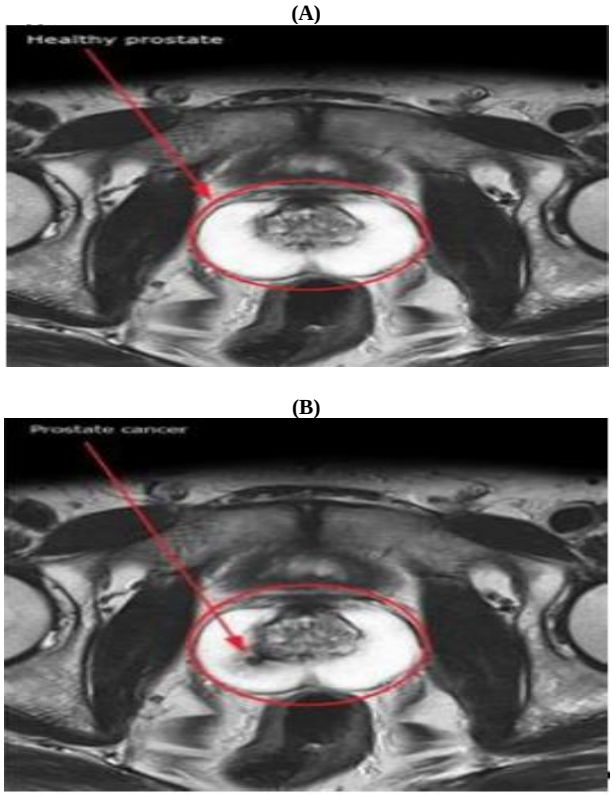

Fig. ١: Prostate MRI Image [1] (A) Sample Image of Prostate Non-Tumor Class(B) Sample Image of Prostate Tumor Class.

The proposed framework consolidates data from two distinct sorts of Magnetic Resonance Images (MRIs), specifically the T2-weighted morphological pictures and the T1-weighted Dynamic Contrast Enhanced (DCE) pictures. Magnetic Resonance Imaging (MRI) uses a widely used medical imaging technique to assess tumors, it is a modern technique that is widely used to detect tumors and is one of the methods that results in high accuracy diagnosis based on the amount of images produced by this technique, while human prediction will not be accurate to give a result about the tumor [1], it is a technique that gives great accuracy in results with minimal damage .

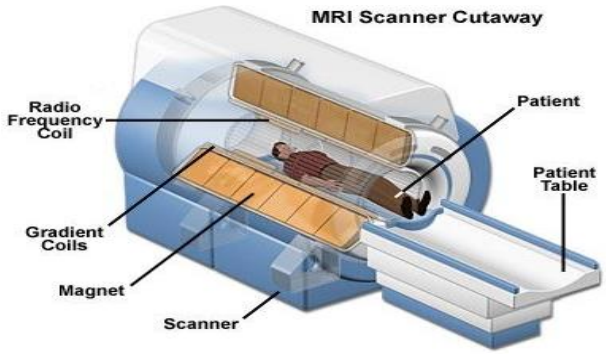

Fig. 2: MRI Scanning [4].

Magnetic resonance imaging (MRI) utilizes a solid attractive field, as well as pulses of wireless frequencies that are connected to the computer to produce detailed images of the body. These images allow doctors to evaluate a different procedure of the body and determine the presence of the disease of non-existent Images are then processed and scanned on the computer screen and are transmitted electronically and then printed or uploaded to a digital cloud server. [4-6].

2. Related work

Many researchers have conducted many studies and researches in medical image to detect prostate tumor based on many methods. According to Hu, X. et al [7] they used artificial neural network for prostate cancer diagnosis and management, they used ANN for evaluating a patient's prostate cancer throughout its history, the general structure of the neural network is forward-forward with backpropagation error to diagnose prostate cancer. during adjustment (training), each neuron adjusts the sum of the balanced inputs with the help of the activation function.

The input layer contains five variables: age of the patient, prostate size and the status of the digital examination of the rectum, % f PSA, and % free PSA the study suggested that the artificial neural network could be used to improve results.

Zhu Y .et al [8] used deep neural networks to extract high-level elemental features to detect prostate cancer based on a hierarchical classification to improve results. Multi-parameter magnetic resonance images were used as inputs to data and based on high-grade acquired traits, hierarchical classification was developed ‹the trials were performed on 21 patients. The proposed method achieves a median assessment based on the sections (SBE) of 89.90%, average sensitivity 91.51%, and mean privacy of 88.47%.

Lemaıtre G. et al [9] They designed a computer-based detection and diagnosis system based on magnetic resonance imaging ‹they used all the MP-MRI modalities for prostate disease detection in your proposed system, MP-MRI CAD system comprises of 7 unique advances: pre-processing, segmentation, registration, feature detection, feature balancing, feature selection/extraction, and finally classification. The different source codes are publicly available, obtained results on a rather complicated dataset of 17 patients with an average AUC of 0.836±0.083 which put our system in the state-of-the-art, even so different CADs were tested on different datasets. In addition, we released the source code and the dataset allowing for reproducibility.

Mehrtasha A. et al [10] proposed framework to use as clinical choice emotionally supportive network to help radiologists in elucidation and announcing of mpMRI.and advancement of a convolution neural network (CNN) model to help CADx in PCa dependent on the presence of prostate tissue in mpMRI,, they saw that 3D CNNs can be efficiently connected for distinguishing clinically significant prostate disease.

Firjani A. et al [11] They proposed a completely new mechanism for the early detection of prostate cancer using DWI the new mechanism to generate color maps showing the proliferation of prostate tissue based on a three-dimensional spatial interaction analysis to change grayscale values. the proposed system prostate segmentation, non-bold registration, and the existing Can-Nyeing classification. For prostate segmentation, the proposed system consists of three main steps. First step Isolation of the prostate from surrounding anatomical structures Depending on the maximum background rating of a new record function, the second step, a non-solid registration algorithm is used to calculate any distortion of the prostate divided by values different b values that can be subject to scanning due to patient respiration and local movement. In the third step, the workbook is used to classify the prostate into benign or malignant based on four aspects of the extracted image. The experimental results on the 28 clinical data collection MRI series yield promising results.

3. Dataset and proposed system

In the proposed framework, we use the data collected by National Center for Photo Therapy Radiology Department, Brigham and Women's Hospital, Harvard Medical School, published on their website. [12]

The data are magnetic resonance images of various cases of prostate tumors for 230 patients, which number more than 1230 images were input on the neural network and trained using Restricted Boltzmann machine algorithm after pre-processing on images,

Prostate images in the dataset are divided into two groups. The first group is Non-tumor prostate images and second group contains images of Tumor prostate as in the table below:

Table 1: Dataset Classification

Non-Tumor Prostate images	Tumor Prostate images	Total images
500	1230	1730

(A)

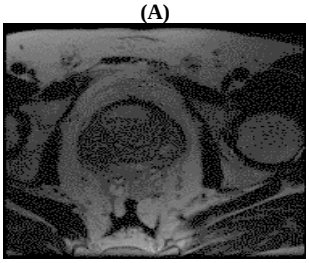

(B)

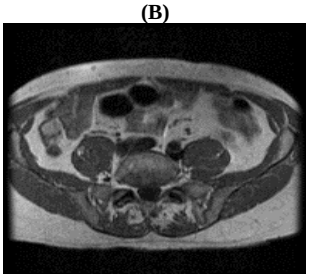

(C)

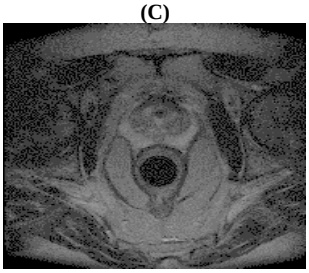

(D)

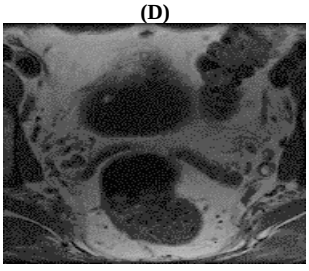

(E)

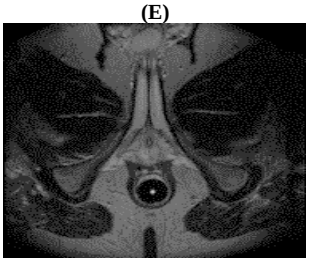

(F)

(G)

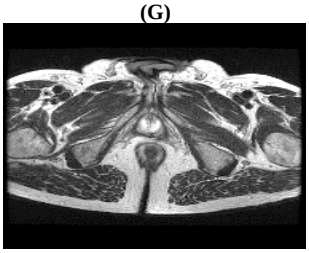

(H)

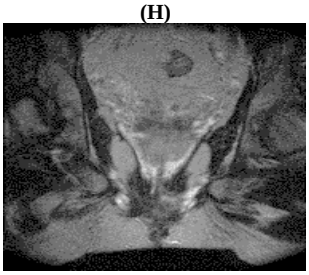

(I)

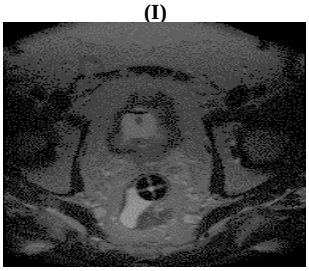

Fig. ٣: Some of MRI Prostate Images Dataset [١2].

The working flow of the proposed framework is appeared in Fig.8 incorporates gathering of the ordinary gathering and irregular gathering information. The collected data are preprocessed and normalized in order to extract quality features. Pre-training and efficient feature set selection from the extracted features is performed. Finally, the selected features are used by the deep belief network classifier to classify tumor in one of the two groups namely Non-tumor group or Tumor group.

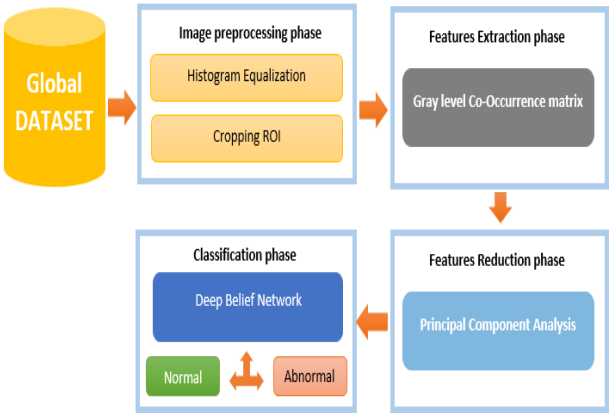

Fig. 4: Block Diagram for Proposed Method.

4. Methodology

4.1. Preprocessing

Preprocessing of MRI images is the primary step of Prostate tumor detection ،In the proposed technique we used histogram equalization one of Contrast enhancement techniques, to enhance grayscale images It improves the difference of images by changing the qualities in a power image with the goal that the histogram of the yield image around matches a predefined histogram, When the contrast is improved the object will be more visible and the

object is easily extracted [13]. This technique supports the next step the feature extraction step.

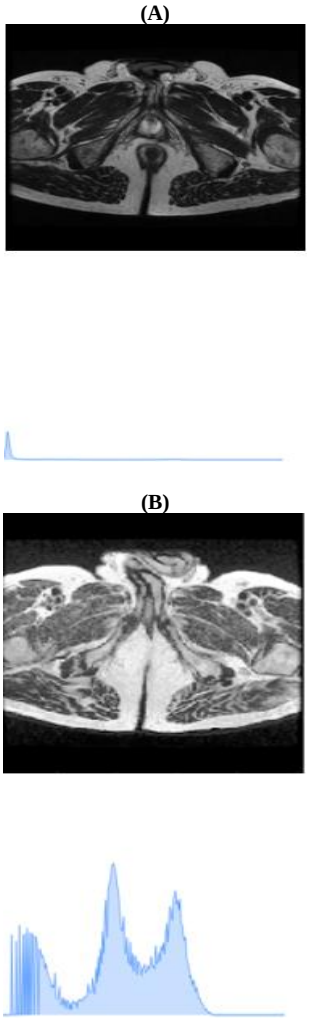

Fig. 5: Show the Pre-Processing Step of the Proposed Model for Non-Tumor Prostate (A) before Histogarm Equalization (B) after Histogram Equalization.

Algorithm 1: Histogram Equalization Filter
Input: Prostate MRI image
Output: MRI image enhanced
Goal: Enhancement contrast
Step1: . Read or peruesd the input image (MRI images)
Step2: Convert the input MRI image into Gray level MRI image
Step3: Apply or perform the Histogram Equalization procedure on the input image (MRI image) to enhance the contrast of the image.
Step4: Take the histogram of enhanced image
Step5: End

After apply histogram equalization , we use Cropping out the region of interest (ROI) ,In this step, the region of interest (ROI) is cropped out from the main images. It is assumed that this ROI is: Rectangular in shape ,Starts at x= 65, y= 62 , It has a height of 152 pixels , It has a width of 148 pixels ,These are the fixed dimensions of image cropping to obtain ROI , the figure below shows this step.

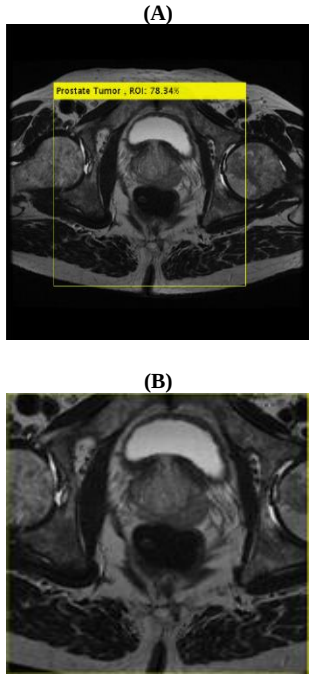

Fig. 6: Cropping Prostate MRI (A) ROI Marked in Yellow (B) Cropped ROI.

4.2. Restricted Boltzmann machines

Restricted Boltzmann machine Is an intelligent neural network based on probability theory an advanced version of the BM invented by Smolensky in 1986 called Harmonium Networks with addition or limitation of determinants. The so-called restrictive is used to simplify learning processes that take time by imposing Boltzmann machine What distinguishes RBM networks is generational and random, generational because it is a generative model of parameters that represents the distribution of probabilities based on observations and training data so that probability distribution (BM fits) with training data by definition [4][14][15][16].

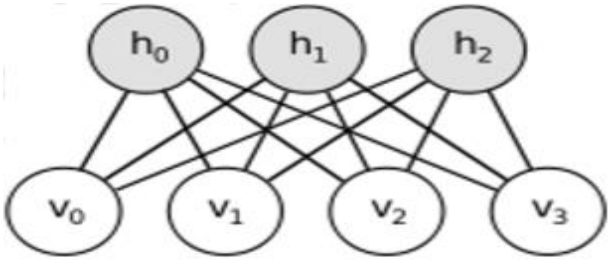

Fig .7: Restricted Boltzmann Machine [3].

The probability distributions over hidden and/or visible units are in terms of the energy function on these configurations: -

$$P(v,h) = \frac{I}{Z} exp\big(-E(v,h)\big) \quad (1)$$

Where Z is:

$$Z = \sum_{v,h} exp(-E(v,h))$$

Then, the maximum likelihood learning algorithm can train the network by simply alternating between updating all the hidden units in parallel and all the visible units in parallel:

$$\frac{\partial log P(v)}{\partial w_{ij}} = < v_i h_j >_0 - < v_i h_j >_\infty \quad (2)$$

Contrastive divergence algorithm is used to fasten the learning for a RBM. In CD algorithm Updating all the hidden units in parallel starting with visible units, reconstruct visible from the hidden

units, and finally update the hidden units again, the learning rule is [4] [14 - 16]:

$$\Delta w_{ij} = < v_i h_j >_0 - < v_i h_j >_1 \quad (3)$$

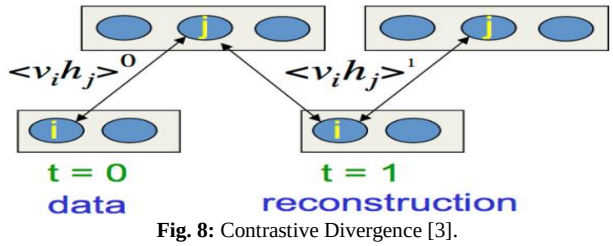

Fig. 8: Contrastive Divergence [3].

Algorithm 2: RBM learning [3]

$RBMupdate(x_1, \in, W, b, c)$

This is the RBM update for binomial units. It can easily adapted to other types of units.
$x_1$is a sample from the training distribution for the RBM ∈ is a learning rate for the stochastic gradient descent in Constrictive Divergence?
W is the RBM weight matrix, of dimension (number of hidden units, number of inputs)
b is the RBM offset vector for input units
c is the RBM offset vector for hidden units
Notation: $Q(h_2 = 1|x_2)$ is the vector with elements $Q(H_{2i} = 1|x_2)$
For all hidden units i do
Compute $Q(h_{1i} = 1|x_1)$ (for binomial units, sigm $(c_1 + \sum_j W_{IJ} x_{ij})$)
Sample $h_{ij} \in \{0,1\}\, from\, Q(h_{1i}|x_1)$
End for
For all visible units i do
Compute $P(x_{2j} = 1|h_1)(for\ binomial\ units, sigm(b_j + \sum_j W_{IJ} h_{1i}))$
Sample $x_{2j} \in \{0,1\}$ from $P(x_{2j} = 1|h_1)$
End for
For all hidden unit ido
Compute $Q(h_{2i}1|x_2)$(for binomial units, $\text{sigm}(c_i + \sum_j W_{ij} x_{2j})$)
End for
$W \leftarrow W + \in (h_i x_1' - Q(h_2 = 1|x_2)x_2')$
$b \leftarrow b + \in (x_1 - x_2)$
$c \leftarrow c + \in (h_1 - Q(h_2 = 1|x_2))$

4.3. Deep belief network (DBN)

Deep Belief Network was presented by Professor Geoffrey Hinton so as to defeat the restrictions of prior neural systems. A profound conviction arrange is a generative realistic model, or even a system of neurons somewhere down in AI type, comprise of a few layers of dormant factors, associations inside the layers, however not inside the units, between each layer
A DBN can figure out how to probabilistically reproduce its data sources when prepared on a lot of precedents in an unsupervised way. The layers at that point go about as highlight indicators on information sources. After this learning venture, to perform grouping, a DBN can be additionally prepared supervisedly.
DBNs can be considered as a straightforward organization of unsupervised system, for example, limited Boltzmann machines (RBMs) or auto encoders, where each sub layer shrouded arrange fills in as the noticeable layer for the following. This likewise prompts a speedy, layer by layer, the unsupervised preparing strategy where the contrastive dissimilarity is connected to each subnet thus, beginning with the 'down' pair of layers (the most reduced obvious layer being a preparation set) [14] [15] [16]

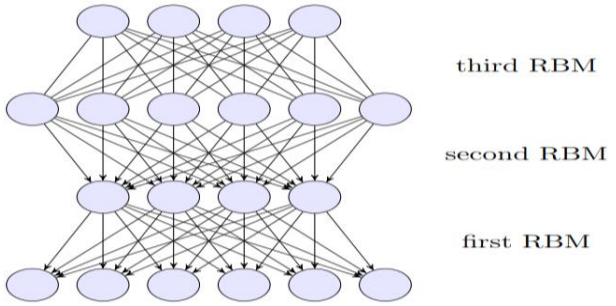

Fig. 9: Deep Belief Network [14].

Contrastive divergence allows us to approximate this for a single layer, and Works to make training time possible, DBN aims to propagate in a different way to representation of the data to each stacked RBM, theoretically this will allow each successive RBM to learn more features in the dataset.
In the DBN Figure 8 when training the first layer of weights, let's assume that the upper layer is used to form a complimentary prior. This assumption reduces this task to training a single RBM, and then passes the data to the next layer by providing a non-linear transformation, to continue training the remaining layers, the dataset is propagated through the first RBM, fixed the first weight matrix This modified dataset is utilized as preparing information for the following RBM, as for the remaining layers above second RBM They will have the same assumptions, his process continues until the top-layer RBM has been trained. Actually, the weighted between the layers is not tied and the number of units in each layer are not alternating as in the figure. [17]

4.4. Feature extraction

Feature extraction phase involves two processes namely data cleaning and data transformation in order to obtain original features set from the prostate data samples. Pre-processing is the major technique used in data cleaning. In the database, there are instances and attributes with noisy values, missing values and duplicate values The extracted feature set with 30 original features is shown in Table 1.
we have used several techniques to extract features and these techniques are: Grey level co-occurrence matrix (GLCM) [18] [19]: Contrast, Correlation, Energy, Entropy, Angular Second Moment, Coarseness 'texture', Skewness, the purpose of using such techniques to obtain the highest accuracy possible and to reduce the error rate. In the proposed system, large data was used. This data contains many variables.

4.4.1. Grey level co-occurrence matrix (GLCM)

discovered by Haralick and others in 1973 is a square matrix that can explore properties about the spatial distribution of gray levels in the texture image, it shows how often the pixel value known as the reference is repeated i occurs in a specific relationship to a pixel value known as a neighboring pixel with Intensity value. Therefore, each element (i, j) of the matrix is the number of times the pixel pair is shown with the value i and a P is the value of j that is at a distance of d for each other. Spatial relationship between the two adjacent Pixels can be selected in many ways through different displacements and angles, where the default setting is pixels

Table 2: Extracted Quality Set of Feature from the Samples of Prostate Data

Prostate data sample features
Grey level co-occurrence matrix & histogram-based features: • Contrast • Correlation • Energy • Entropy • Angular Second Moment Coarseness 'texture' • Skewness

And pixels the immediate neighbor to the right. [18 - 21].

Algorithm 3: GLCM Feature extraction
Input: MRI images for non-tumor Prostate and tumor Prostate
Output: Texture feature vector
Goal: GLCM feature extraction
Step 1: Reading MRI Images
Step 2: Count all pairs of pixels in which the first pixel has a value i, and its matching pair displaced from the first pixel by d has a value of j.
Step 3: This count is entered in the ith row and jth column of the matrix Pd[i,j]
Step 4: Note that Pd[i,j] is not symmetric, since the number of pairs of pixels having gray levels[i,j]does not necessarily equal the number of pixel pairs having gray levels [j,i].
Step 5: The elements of Pd[i,j]can be normalized by dividing each entry by the total number of pixel pairs.
Step 6: Normalized GLCM N[i,j], defined by:

4.4.2. Contrast [18-19]

The contrast is the frequency of the pixel pair and determines spatial spatiality. Is divided into several gray G levels and stores the concurrent probabilities of gij to determine the properties of the fabric, through the repetition on the entire matrix the statistics are selected and applied to each GLCM.

$$(\text{con}) = \sum_i \sum_j (i-j)^2 g_{ij} \quad (4)$$

Text features are based on statistics that summarize the relative frequency distribution that describes how often a gray tone will appear in a specific spatial relationship with another gray color on the image.

This measurement measures the spatial recurrence of an image and is contrast minute of GLCM. It is the contrast between the most elevated and the lowest values of a bordering set of pixels. It measures the amount of local variations present in the image. A low contrast image presents GLCM concentration term around the principal diagonal and features low spatial frequencies.

4.4.3. Correlation [18] [19]

$$(\text{cor}) = \frac{\sum_i \sum_j (ij) g_{ij} - \mu\mu_x\mu_y}{\sigma_x \sigma_y} \quad (5)$$

where μ_x, μ_y, σ_x and σ_y are the means and standard deviations of g_x and g_y The correlation feature is a measure of gray tone linear dependencies in the image. The rest of the textural features are secondary and derived from those listed above.

4.4.4. Energy [18] [19]

$$(\text{ene}) = \sum_i \sum_j g_{ij^2} \quad (6)$$

This measurement is additionally called Consistency or Precise moment minute. It measures the textural consistency that's pixel match reiterations. It identifies disarranges in surfaces. Vitality comes to a greatest esteem rise to to one.

4.4.5. Entropy [18]

$$(\text{ent}) = -\sum_i \sum_j g_{ij} \log_2 g_{ij} \quad (7)$$

This statistic measures the disorder or complexity of an image. The entropy is large when the image is not texturally uniform and many GLCM elements have very small values. Complex textures tend to have high entropy. Entropy is strongly, but inversely correlated to energy.

Table 3: The Feature Vector to A Sample of the Non-Tumor Prostate vs. Tumor Prostate Image

MRI Image	Grey level co-occurrence matrix (GLCM)& Histogram Based Features						
	Contrast	Correlation	Energy	Entropy	Angular Second Moment	Coarseness	Skewness
Image (Non-Tumor)	0.1203	0.1391	0.7439	0.6915	0.1262	0.1150	0.8308
	0.2017	0.1882	0.8055	0.7986	0.0674	0.0712	0.9777
	0.1120	0.1422	0.8327	0.7659	0.1253	0.1130	0.8667
	0.4240	0.4648	0.8228	0.7865	0.1102	0.1158	0.7107
	0.3578	0.4496	0.8912	0.8434	0.2569	0.2598	0.6842
	0.4768	0.5301	0.8055	0.7423	0.1104	0.1075	0.6835
	0.6363	0.6488	0.7861	0.6242	0.0216	0.0087	0.6091
	0.1273	0.7951	0.6444	0.5322	0.0107	0.1117	0.6010
	0.1178	0.1432	0.8055	0.7389	0.1204	0.1068	0.8623
	0.1210	0.1395	0.5862	0.7266	0.1233	0.0763	0.8096
Image (Tumor)	0.1248	0.1033	0.8614	0.8761	0.1467	0.1521	0.6653
	0.1349	0.1183	0.8547	0.8638	0.0924	0.1013	0.6780
	0.3198	0.2958	0.8419	0.8425	0.0282	0.0287	0.8472
	0.2766	0.2997	0.8607	0.8301	0.0320	0.0287	0.8833
	0.1936	0.3003	0.8777	0.7730	0.0902	0.0688	0.8919
	0.1927	0.1867	0.6926	0.6898	0.0711	0.0709	0.7337
	0.1928	0.1886	0.7146	0.7117	0.0740	0.0782	0.7566
	0.2591	0.2186	0.6857	0.7274	0.0467	0.0570	0.8055
	0.2164	0.2146	0.7660	0.7541	0.0508	0.0547	0.8389
	0.2390	0.2316	0.7833	0.7752	0.0500	0.0531	0.8745

In order to reduce the number of variables, while preserving the information in the original dataset, Principal component analysis (PCA) The best techniques widely used, is one of the statistical methods used on a wide field in computer science, [22] [23]. Most prostate statistical modelling techniques are based on the principal component analysis method [24]. PCA used to reduce the dimension and reduce the complexity of the data set while reducing the loss of information. It is a powerful way to represent data because it has the ability to capture the most variable data components of samples [41]. see figure 10

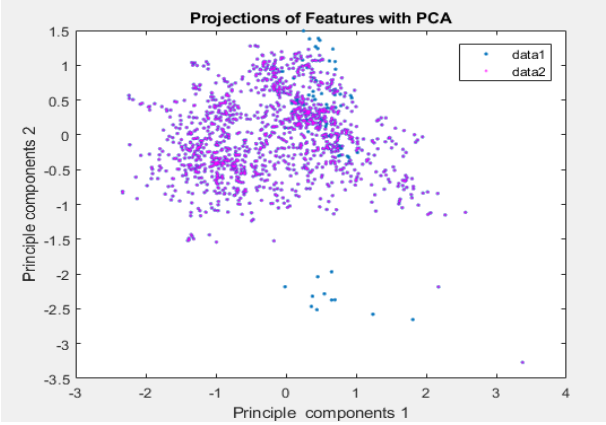

Fig. 10: Show the Projections of Features with Principle Component Analysis.

5. Implementation using neural network

For the purpose of comparison and validation of the proposed system, we introduced the dataset in the table 1 [12], into the neural network and trained the network

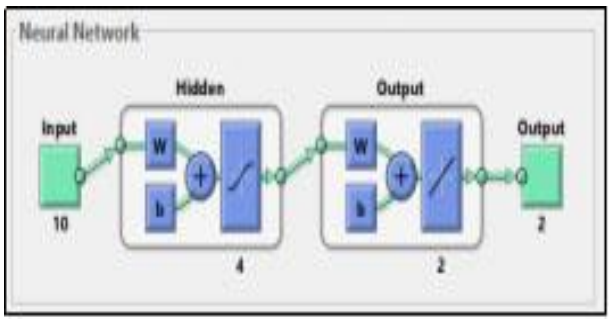

Fig. 11: Show Neural Network Model by MATLAB.

The problem under evaluation is binary classification, the parameters used for weight are accuracy, quality and sensitivity. These parameters are defined as follows [25]:

Sensitivity = TP / TP + FN × 100

Specificity = TN / TN + FP × 100

Precision = TP + TN / TP + TN + FP + FN × 100

When TP is True positive, TN is true negative, and FP and FN are both false and negative respectively. The sensitivity measures the percentage of the cancer layer expected to be real, and the specificity of the percentage of the natural layer is really predicted, and the accuracy is the percentage of cancer expected correctly and normal cases , the accuracy is 93,8% Data is rotated many times and the best result is shown in the matrix of confusion below.

Fig. 12: Show Confusion Results for Neural Network.

Graphical representation of performance of the neural network is represented in the figure 11 where, 104 epoch of learning process, the network has shown its best performance of validation with a value of 19.412. Below in figure 13, the best validation performance when the epoch 104, the number of epoch 110.

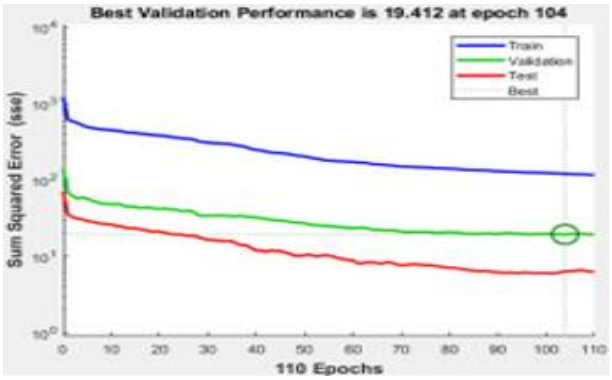

Fig. 13: Show Best Validation Performance for Neural Network.

The training state in the neural network at epoch 110, the Gradient is 33.31, figure 14 show this results.

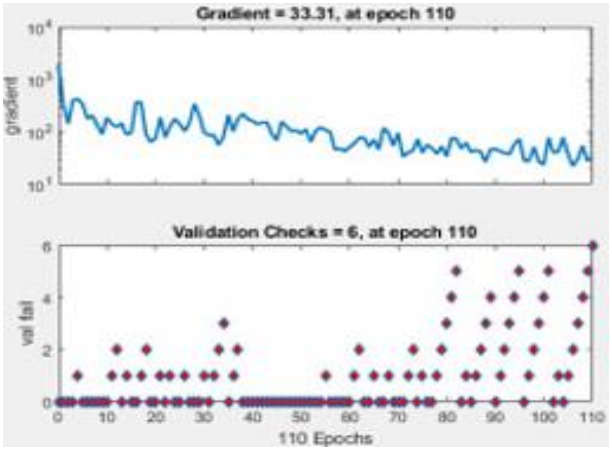

Fig. 14: Show Training State in Neural Network.

6. Proposed system implementation and results

Preparing a RBM with Contrastive Uniqueness calculation requires a certain number of cycles to merge into an ideal esteem. A disappointment to get an ideal esteem for each RBM comes about in destitute execution of in general framework since RBM may be a fundamental building piece of DBN. Probably, it shows up running various cycles yields superior comes about, but in reality, it does not as it were take a long time to prepare, but it moreover closes up over-fitting the information. As a result, it is critical to halt some time recently the over-fitting happens.

In this paper, the DBN trained for 1000 epochs continuously improves for the duration of 2000 epochs; however, it clearly shows it has higher errors than the DBN trained for 2000 epochs. The DBN trained for 3000 epochs already has much better performance at 1000 epochs. Nevertheless, the graph starts to gradually increase, which hints the sign of overfitting, the table 2 show this results The DBN algorithm was chosen and programmed in MATLAB for its ease in representing the visual and hidden layers as well as the weights, which are represented as arrays and the implementation of algorithms with high efficiency. DBN consists of several layers of RBM so the basis of DBN is RBM so the implementation of DBN includes the training of each layer RBM, initially we randomly set up the units for the purpose of training RBM and there are two positive and negative phases are there in Contrastive Divergence Algorithm When calculating the potential weights and visual units during the positive phase, the binary cas-

es of the hidden units are identified. The positive phase is called the positive phase because it increases the probability of the training data. In contrast to the positive phase, the probability of the enzymes produced by the negative phase is reduced. At the end of the experiment, Model, and the actual vector of data. In the end, the visual unit derivations are taken with respect to weights. This is the expectation of the difference between the positive and negative phases of the weighting. After calculating the error, to train the whole DBN, the machine used for conducting this experiment is configured with 4 GB RAM memory and Intel(R) Core(TM) i7 1.80 GHz processor. The neural network was designed with hidden layers and size [٥ ٢٠] figure (14) show the DBN structure. We were trained in high efficiency during record time. We obtained 98.8439 accuracy and Mean Squared Error 0.0115.

Table 4: Show Results with Different Hidden Layer Size

Architecture	Accuracy %	MSE %	Precision %
10 -10	90.7514	0.0924	0.0980
20 - 5	98.8439	0.0115	0.9801
30 - 40	93.4489	0.9741	0.0655
100 - 100	71.0983	0.2890	NAN

The RBM-based prostate cancer detection algorithm is successfully applied to MRI images, and at high accuracy.
Figure (15) below show the DBN structure of our approach.

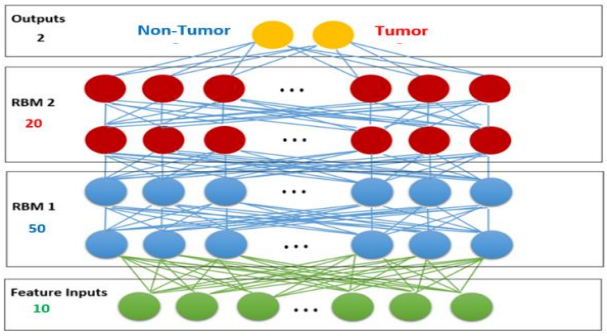

Fig. 15: DBN Structure of Proposed Method.

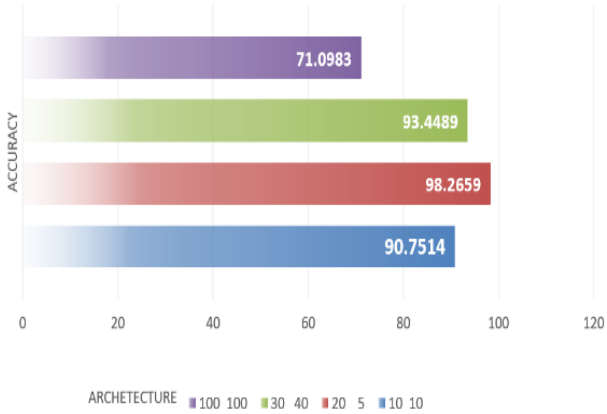

Fig. 16: Show the Accuracy with Different Network Architecture.

7. Conclusion and future scope

The proposed system shows that the application of RBM for feature selection and DBN for classification achieves better results and performance in the classification of prostate tumors. The proposed system obtains higher detection rate than the models used in the existing systems. Use Deep Belief Network that uses directed links of the neural units among the visible and hidden layers, a deep learning approach, is an innovative step taken in the proposed model. The future work Additional other deep learning algorithms like Convolutional Neural Networks, Stacked Auto Encoder, etc. can be used in the prostate tumor prediction and classification and developed proposed system to classify the tumor into benign and malignant.

References

[1] Banerjee, S., & Kaviani, A. (2016). Worldwide prostate cancer epidemiology: Differences between regions, races, and awareness programs.

[2] Center, M. M., Jemal, A., Lortet-Tieulent, J., Ward, E., Ferlay, J., Brawley, O., & Bray, F. (2012). International variation in prostate cancer incidence and mortality rates. *European urology*, *61*(6), 1079-1092. https://doi.org/10.1016/j.eururo.2012.02.054.

[3] Lemaitre G., Martí R., et al. "Computer-Aided Detection for Prostate Cancer Detection based on Multi-Parametric Magnetic Resonance Imaging" EMBC2017: 39th Annual International Conference of the IEEE Engineering in Medicine and Biology Society, Jul 2017, Jeju Island, South Korea.

[4] Thahseen P, Anish Kumar B, "A Deep Belief Network Based Brain Tumor Detection in MRI Images", International Journal of Science and Research (IJSR), Vol. 6,2015, pp. 495 ,498.

[5] Radiological Society of North America, "Magnetic Resonance Imaging (MRI) – Body", June 2018, http://www.radiologyinfo.org.

[6] Ampeliotis, D., Antonakoudi, A., Berberidis, K., Psarakis, E. Z., & Kounoudes, A. (2008, March). A computer-aided system for the detection of prostate cancer based on magnetic resonance image analysis. In Communications, Control and Signal Processing, 2008. ISCCSP 2008. 3rd International Symposium on (pp. 1372-1377). IEEE. https://doi.org/10.1109/ISCCSP.2008.4537440.

[7] Hu, X., Cammann, H., Meyer, H. A., Miller, K., Jung, K., & Stephan, C. (2013). Artificial neural networks and prostate cancer—tools for diagnosis and management. *Nature Reviews Urology*, *10*(3), 174. https://doi.org/10.1038/nrurol.2013.9.

[8] Zhu, Y., Wang, L., Liu, M., Qian, C., Yousuf, A., Oto, A., & Shen, D. (2017). MRI-based prostate cancer detection with high-level representation and hierarchical classification. *Medical physics*, *44*(3), 1028-1039. https://doi.org/10.1002/mp.12116.

[9] Lemaitre, G. (2016). *Computer-aided diagnosis for prostate cancer using multi-parametric magnetic resonance imaging* (Doctoral dissertation, Ph. D. dissertation, Universitat de Girona and Université de Bourgogne).

[10] Mehrtash, A., Sedghi, A., Ghafoorian, M., Taghipour, M., Tempany, C. M., Wells, W. M., ... & Fedorov, A. (2017, March). Classification of clinical significance of MRI prostate findings using 3D convolutional neural networks. In *Medical Imaging 2017: Computer-Aided Diagnosis* (Vol. 10134, p. 101342A). International Society for Optics and Photonics.

[11] Firjani, A., Khalifa, F., Elnakib, A., Gimel'farb, G., El-Ghar, M. A., Elmaghraby, A., & El-Baz, A. (2012, September). A novel image-based approach for early detection of prostate cancer. In *Image Processing (ICIP), 2012 19th IEEE International Conference on* (pp. 2849-2852). IEEE. https://doi.org/10.1109/ICIP.2012.6467493.

[12] The Ferenc Jolesz National Center for Image Guided Therapy, Harvard medical school, Brigham and woman school," Prostate MR Image Database", 2008, http://prostatemrimagedatabase.com/index.html.

[13] Musthofa Sunaryo et al, "Preprocessing on Digital Image using Histogram Equalization: An Experiment Study on MRI Brain Image / (IJCSIT) International Journal of Computer Science and Information Technologies, Vol. 7 (4) 2016, 1723-1727.

[14] Hebbo H., Won Kim J, "Classification with Deep Belief Networks".

[15] Hinton, G. E. (2012). A practical guide to training restricted Boltzmann machines. In Neural networks: Tricks of the trade (pp. 599-619). Springer, Berlin, Heidelberg https://doi.org/10.1007/978-3-642-35289-8_32.

[16] Fischer A., Igel CH., "An Introduction to Restricted Boltzmann Machines", (Eds.): CIARP 2012, LNCS 7441, pp. 14–36, 2012 https://doi.org/10.1007/978-3-642-33275-3_2.

[17] Sims, James Christopher, "An Implementation of Deep Belief Networks Using Restricted Boltzmann Machines in Clojure" (2016). Open Access Master's Theses. Paper 804. http://digitalcommons.uri.edu/theses/804.

[18] Sebastian V B., Unnikrishnan A, et al." Grey Level Co-occurrence Matrices: Generalisation and some new features ", International Journal of Computer Science, Engineering and Information Technology (IJCSEIT), Vol.2, No.2, April 2012.

[19] Pathak B, Barooah D, "Texture Analysis Based on the Gray-Level Co-Occurrence Matrix Considering Possible Orientations, International Journal of Advanced Research in Electrical, Electronics and Instrumentation Engineering,Vol. 2, September, 2013.

[20] Grakari DH, "Image Quality Analysis Using GLCM MSc. Thesis, University of Central Florida, Orlando, Florida, 2004.

[21] Sharma, E. K., Priyanka, E., Kalsh, E. A., & Saini, E. K. GLCM and its Features.
[22] Song, F., Guo, Z., & Mei, D. (2010, November). Feature selection using principal component analysis. In System science, engineering design and manufacturing informatization (ICSEM), 2010 international conference on (Vol. 1, pp. 27-30). IEEE. https://doi.org/10.1109/ICSEM.2010.14.
[23] Yang, L. (2015). An application of principal component analysis to stock portfolio management.
[24] Chilali, O., Ouzzane, A., Diaf, M., & Betrouni, N. (2014). A survey of prostate modeling for image analysis. Computers in biology and medicine, 53, 190-202. https://doi.org/10.1016/j.compbiomed.2014.07.019.
[25] Haifeng Wang. "Ensemble learning approach for classification variance reduction in breast cancer diagnosis". MSc. Thesis, Binghamton University, State University of New York, ProQuest LLC. 2015.